

# Kinetic Description of the Hydrogenation of Nitrobenzene and Nitrosobenzene on Skeletal Nickel in Aqueous Solutions of Propan-2-ol of Different Compositions

Yu. E. Romanenko\*, A. A. Merkin, and O. V. Lefedova\*\*

Research Institute of Thermodynamics and Kinetics of Chemical Processes,  
Ivanovo State University of Chemistry and Technology, Ivanovo, 153000 Russia

\*e-mail: Romanenko@isuct.

\*\*e-mail: physchem@isuct.ru

Received July 5, 2014; in final form, June 12, 2015

**Abstract**—The kinetics of the hydrogenation of nitrosobenzene and nitrobenzene is simulated taking into account accompanying processes and specific features of the conversion of reactive groups. The constants of the hypothetical reaction steps are calculated. The influence of sodium hydroxide and acetic acid on the kinetic parameters of the reactions is discussed.

**Keywords:** nitrobenzene, nitrosobenzene, skeletal nickel, propan-2-ol, sodium hydroxide, acetic acid, kinetic modeling

**DOI:** 10.1134/S0023158416020117

## INTRODUCTION

Discussing the stepwise character of the conversion of nitrobenzenes during their hydrogenation, different authors noted that the conversion of the nitro group is accompanied by the consecutive addition of hydrogen and the formation of phenylhydroxylamine and nitroso-, azoxy-, and azobenzenes, depending on the reaction conditions [1, 2]. The studies showed that the hydrogenation of substituted nitrobenzenes is accompanied by a series of side processes, such as catalyst surface oxidation and solvent dehydrogenation. The competitive character of the adsorption of the starting compounds and reaction products cannot be excluded [3, 4]. These processes should be taken into account in the development of kinetic models.

Poor attention is presently given to development of kinetic models for liquid-phase hydrogenation processes. There are several published descriptions of the hydrogenation of substituted benzenes, in particular, on platinum [2, 5] and skeletal nickel [6–8]. However, no calculations were performed using the proposed models, except in our earlier study [8].

The purpose of this work is to substantiate the kinetic models of the reduction of nitrobenzene and nitrosobenzene taking into account the specific features of the conversion of the nitro and nitroso groups and the processes accompanying hydrogenation, such as catalyst surface oxidation and solvent dehydrogenation.

## EXPERIMENTAL

Skeletal nickel to be used as the catalyst was prepared by treating a nickel–aluminum alloy (Ni : Al :

Fe = 47.5 : 50.2 : 0.3 (wt %), average particle radius of 4.5–4.8  $\mu\text{m}$ ) with an aqueous solution of sodium hydroxide using a standard procedure [9]. The active catalyst had the specific surface area and porosity of  $90 \pm 2 \text{ m}^2/\text{g}$  and  $0.5 \pm 0.06 \text{ cm}^3/\text{cm}^3 \text{ Ni}$ , respectively [9].

An aqueous solution of propan-2-ol of the azeotropic composition ( $x_2 = 0.68 \text{ ppm}$ ) was used as the solvent. The catalyst weight was  $0.500 \pm 0.005 \text{ g}$ , and the amounts of nitrosobenzene and nitrobenzene in the reactor were  $8.18 \pm 0.02$  and  $12.80 \pm 0.2 \text{ mmol}$ , respectively.

The kinetics of hydrogenation over skeletal nickel were studied by the static method in a closed reactor with a vigorously stirred liquid phase at  $T = 303 \pm 1 \text{ K}$  using an earlier described procedure [9]. The experiments were carried out with a continuous hydrogen supply in such a way that the hydrogen pressure was be 1 atm. The catalyst was preliminarily loaded into the reactor filled with the solvent, its surface was saturated with hydrogen, and then a nitroso compound was added. With this component mixing sequence, the amount of hydrogen adsorbed on the catalyst was maximum for the given temperature and solvent composition. The experimental conditions excluded the influence of the external mass transfer on the reaction rate, and the starting reactant concentration range in which the reaction was performed ensured a high rate of saturation of the catalyst surface with hydrogen. The hydrogen uptake in the course of time, which quantitatively characterized the totality of catalytic conversions taking place, was measured volumetrically.

## COMPUTATIONAL PROCEDURE

The rate constants for hydrogen adsorption on the nickel catalyst surface and for propan-2-ol dehydrogenation were found from the experimental data, and the adsorption equilibrium constant was determined from an aniline adsorption isotherm [3]. The adsorption constants of phenylhydroxylamine and azoxy-, azo-, and hydrazobenzenes as well as the constants of the reactions of these compounds with hydrogen in the surface layer were obtained by simulation [4]. Thus, when developing the model, some constants were calculated from our experimental data and others were determined using published data.

The changes in the concentrations of the starting compounds, intermediates, and reaction products in time were calculated earlier using UV and IR spectroscopy, liquid chromatography, and GLC data [10]. Azoxybenzene concentrations were determined on a CARY 50 scan UV-Visible Spectrophotometers spectrophotometer (Varian, Australia) in a wavelength range of 240–500 nm using quartz cells with an optical path of 1 cm and the pure solvent as the reference sample. The concentrations of nitrobenzene and aniline were calculated from GLC data obtained on an LKhM-80.6 chromatograph (Russia) with a flame-ionization detector and a 1.5-m-long packed column (solid phase Chromaton N-AW (400–600  $\mu\text{m}$  fraction) with supported Lukopren G-1000 (7 wt %), oven temperature of 451 K, injection port temperature of 593 K, detector temperature of 513 K, He as the carrier gas (2.50 atm)). The concentrations of nitrobenzene, nitrosobenzene, and phenylhydroxylamine were measured on an LC-6A liquid chromatograph (Shimadzu, Japan) equipped with a spectrophotometric detector with deuterium and tungsten lamps (220–500 nm) and a stainless steel packed column (25 cm, oven temperature of 303.5 K, solid phase Lichrosorb RP-18 (5  $\mu\text{m}$  fraction)) using aqueous solutions of acetonitrile as the eluent (30 wt %, eluent flow rate 0.9  $\text{cm}^3/\text{min}$ ) and a sample injector.

The reproducibility of experimental data was determined from the results of a series of experiments on the liquid-phase hydrogenation of each of the compounds. Each experiment was repeated 3–5 times in such a way that the initial amounts of the hydrogenated compound differed by no more than 0.5% and the difference between the sampling times in repeated injections did not exceed 2–3 s.

The average value of the measured parameter was calculated for each time interval, and then the averaged reproducibility variance ( $S_y^2$ ) was determined via the equation

$$S_{y_i}^2 = \sum_{j=1}^{m_i} (n_{ij} - \bar{n}_i)^2 / (m_i - 1),$$

where  $m_i$  is the number of replica experiments at the  $i$ th point in time,  $n_{ij}$  is the amount of the compound

determined at the  $i$ th point in time in the  $j$ th experiment, and  $\bar{n}_i$  is the average value over all experiments.

The adequacy of the proposed model to experimental data was checked in terms of three independent parameters: changes in the amounts of the starting compound and the reaction product in the solution bulk and the amount of hydrogen absorbed from the gas phase as functions of time. The goodness of fit between the calculated and experimental values was estimated using Fischer's criterion, whose values were calculated on the basis of the averaged reproducibility variance and residual variance ( $S_{\text{res}}^2$ )

$$S_{\text{res } j}^2 = \sum_{i=1}^q (n_{ij}^{\text{exp}} - n_{ij}^{\text{calc}})^2 / (q - r),$$

where  $q$  is the number of measurements, and  $r$  is the number of constants estimated in the model.

The checking of the hypothesis about the equality of the variances using the indicated criterion showed that the difference between the residual variance and the reproducibility variance was statistically insignificant at a confidence probability of  $p = 1 - \alpha = 0.95$ .

The following assumptions were accepted for the development of the kinetic schemes:

- the conversions proceed via the Langmuir–Hinshelwood adsorption mechanism;
- the reversible adsorption of the hydrogenated compound, reaction product, and intermediate compounds occurs on the active sites  $Z$ , and hydrogen is adsorbed on the sites  $Y$ ;
- hydrogen adsorption involves one active site of the catalyst surface, and the possibility of hydrogen migration in the surface layer is excluded;
- the starting compounds react irreversibly with hydrogen;
- the activated adsorption of the starting and intermediate compounds on the active sites of the catalyst surface can be accompanied by the oxidation of the latter;
- there can be both the reversible and irreversible oxidation of the active sites of the catalyst surface;
- the solvent can undergo reversible dehydrogenation, and the resulting hydrogen can participate in the reduction of reactive groups.

The following conditions were fulfilled at each stage of the calculations:

- no more than 30% of the constants were varied in the model calculations;
- the constants determined from experimental or earlier published data and those calculated for simpler schemes were varied within one order of magnitude;
- the constants of the steps that were not rate-determining were related to other constants by certain equations;
- the rate constants of the reversible steps included in the kinetic schemes were calculated from adsorption equilibrium constants;

**Table 1.** Rate constants corresponding to the optimum calculations according to the model of nitrosobenzene reduction on skeletal nickel in an aqueous solution of propan-2-ol ( $x_2 = 0.68$ )

Step	Rate constants of steps*	Solvent		
		without additives	0.01 M CH <sub>3</sub> COOH	0.01 M NaOH
I	$k_1 \times 10^2, \text{m}^3 \text{mol}^{-1} \text{s}^{-1}$	$3 \pm 1$	$3 \pm 1$	$3 \pm 1$
	$k_1/k_2, \text{m}^3 \text{mol}^{-1}$	$3.8 \pm 0.2$	$3.8 \pm 0.2$	$3.8 \pm 0.2$
II	$k_3 \times 10^2, \text{m} \text{mol}^{-1} \text{s}^{-1}$	$0.8 \pm 0.4$	$0.4 \pm 0.08$	$3 \pm 1$
	$k_3/k_4, \text{m}^3 \text{mol}^{-1}$	(10)	(10)	(10)
III	$k_5 \times 10^2, \text{m}^3 \text{mol}^{-1} \text{s}^{-1}$	(50)	(0.02)	(0.5)
	$k_5/k_6, \text{m}^3 \text{kg mol}^{-2}$	(0.1)	(0.1)	(0.1)
IV	$k_7 \times 10^2, \text{m}^3 \text{mol}^{-1} \text{s}^{-1}$	(2)	(0.02)	(0.1)
	$k_7/k_8 \times 10^2, \text{m}^3 \text{mol}^{-1}$	(1)	(0.05)	(0.1)
V	$k_9, \text{kg mol}^{-1} \text{s}^{-1}$	$5 \pm 1$	$2 \pm 0.3$	$5 \pm 1$
	$k_{10}, \text{kg mol}^{-1} \text{s}^{-1}$	$0.9 \pm 0.05$	$0.9 \pm 0.4$	(3)
	$k_{11} \times 10^2, \text{kg mol}^{-1} \text{s}^{-1}$	$7 \pm 2$	$4 \pm 2$	(70)
	$k_{12} \times 10^2, \text{kg mol}^{-1} \text{s}^{-1}$	$7 \pm 2$	$3 \pm 1$	$3 \pm 1$
VI	$k_{13} \times 10, \text{kg mol}^{-1} \text{s}^{-1}$	$4 \pm 1$	$1.5 \pm 0.6$	$15 \pm 5$
	$k_{14}, \text{kg mol}^{-1} \text{s}^{-1}$	$50 \pm 15$	$9 \pm 3$	$120 \pm 40$
VII	$k_{15} \times 10^3, \text{s}^{-1}$	$3.3 \pm 0.2$	—	$4.5 \pm 2$
	$k_{15}/k_{16}, \text{mol m}^{-3}$	7.3	—	7.3

Estimated values are given in parentheses. Dashes in the columns mean that this step did not contribute noticeably to the overall reaction rate.

\* The dimensions of the constants depend on the dimensions of the concentrations.

(e) the differential equations corresponding to the proposed stepwise mechanism of the conversion of one reactive group or another were solved by numerical methods without using other assumptions;

(f) the concentration of propan-2-ol was taken into account in the corresponding rate constant, since in the course of the reaction this concentration exceeded those of the starting compound and acetone by approximately four orders of magnitude.

## RESULTS AND DISCUSSION

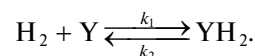
When comparing kinetic models, data on the adsorption of hydrogen [10, 11], nitrobenzene, and intermediate products of nitro group reduction [10] and on the kinetics of propan-2-ol dehydrogenation [3] were used and the stepped character of nitrobenzene conversion during hydrogenation [1, 2, 10] was taken into account. The rate constants of individual steps, which were subsequently used in the construction of the kinetic schemes and in the simulation of the hydrogenation of nitrobenzene (NB) and nitrosobenzene (NS), were calculated from published data [11–13].

According to the literature [1, 2], NS is one of the intermediates of nitro group reduction. The nitroso group can be further converted through the formation of either azoxybenzene (AZOB) [1] or phenylhydroxylamine (PHA) [2]. It is believed [12] that NS has the highest oxidation potential among the products of the incomplete reduction of the nitro group. An analysis of experimental data [12] indicates that dehydrogenation occurs most actively on the oxidized catalyst surface. When choosing steps of the conversion of the hydrogenated compounds, we used approaches similar

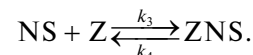
to the description of the hydrogenation kinetics of other intermediates of nitro group reduction, namely, PHA and azobenzene (AB) [14].

The following NS conversion steps were accepted on the basis of the above statements. The set of steps additionally included two independent routes of the reduction of the starting compound, one through PHA and the other through AZOB, followed by the formation of AB and hydrazobenzene (HAB). The possibility of solvent (SH<sub>2</sub>) dehydrogenation to acetone (S) was also taken into account. It was assumed that hydrogen and organic compounds were adsorbed on the sites Y and Z, respectively.

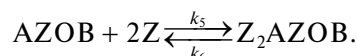
I. Adsorption of hydrogen on the catalyst surface:



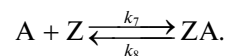
II. Adsorption of NS on the catalyst surface:



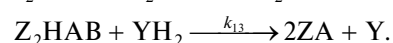
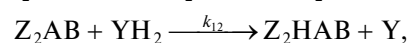
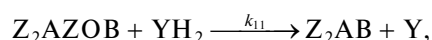
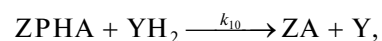
III. Adsorption of AZOB on the catalyst surface:



IV. Adsorption of aniline (A) on the catalyst surface:

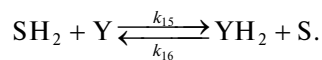


V. Chemical interaction in the surface layer:



VI. Formation of oxidized sites  $Z^{\text{ox}}$ :

## VII. Reversible dehydrogenation of the solvent:



The constants  $k_1$  and  $k_{15}$  and the ratio  $k_7/k_8$  were estimated from experimental data. The constant  $k_7$  and the ratios  $k_1/k_2$  and  $k_{15}/k_{16}$  were published [10, 11], and the constants  $k_5$ ,  $k_6$ , and  $k_{10}-k_{13}$  were found earlier for the description of PHA hydrogenation [14]. The constants  $k_3$ ,  $k_4$ ,  $k_9$ ,  $k_{10}$ , and  $k_{14}$  were varied and were determined in the course of simulation, and the constant  $k_{10}$  was changed only in the systems with an acid or base additive. The values of the constants providing the best fit between the experimental and calculated values are given in Table 1.

The results of calculations using the model describing NS conversion during hydrogenation on skeletal nickel in aqueous solutions of propan-2-ol of different compositions are presented in Fig. 1.

The exclusion of the steps of solvent oxidation and dehydrogenation from the general kinetic scheme resulted in significant discrepancies between the calculated and experimental data. This exerted the strongest effect on the time dependence of the hydrogen uptake. Thus, it can be assumed that the contribution from the oxidation and reversible dehydrogenation of the solvent to the overall rate of NS hydrogenation is more significant than in the earlier considered variants of calculations for other intermediate products of NB reduction, namely, PHA and AB [14].

The simulation results did not exclude the variant of simultaneous AZOB and PHA formation from semihydrogenated intermediates, whose structures were proposed earlier [1]. The best fit between the experimental and calculated values is achieved under the condition that AZOB is predominantly formed due to oxidation processes (step VI) and PHA is formed due to interactions with adsorbed hydrogen. The assumption that the nitroso group can be converted only through AZOB formation leads to significant discrepancies between the experimental and calculated dependences.

The results of the simulation of NS hydrogenation confirmed the hypothesis that the contribution from the oxidation processes to the overall reaction rate increases in the presence of sodium hydroxide. For

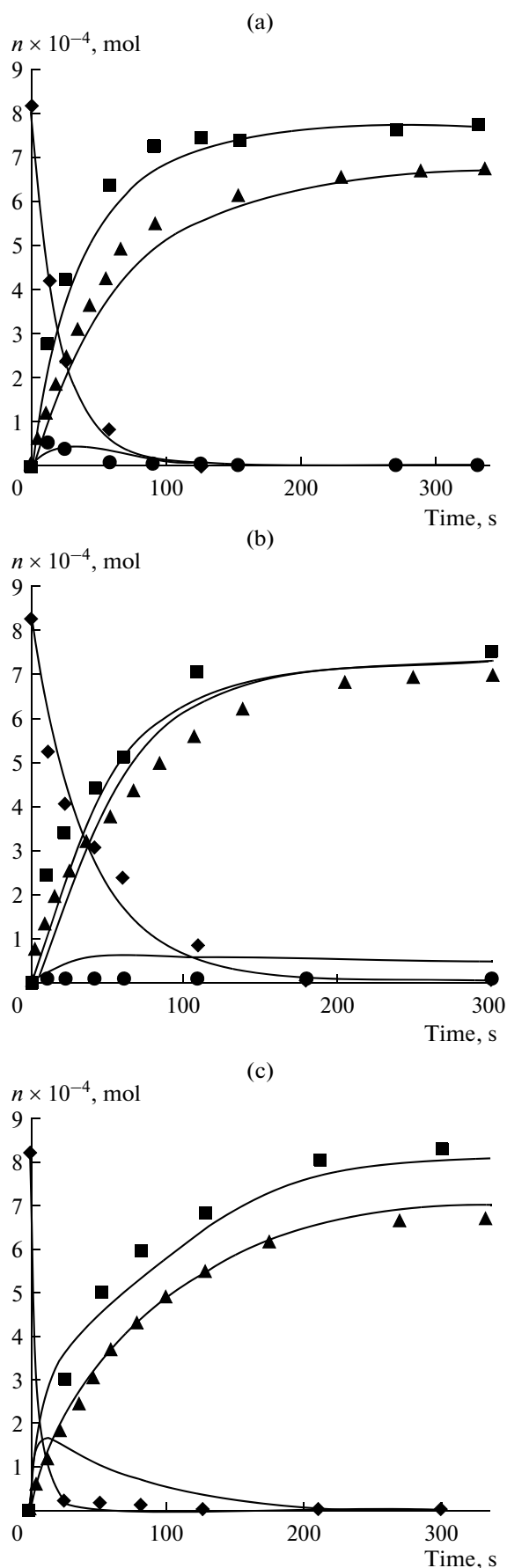


**Fig. 1.** Amounts of (♦) nitrosobenzene, (●) azoxybenzene, (■) aniline, and (▲) hydrogen absorbed from the gas phase taking into account the stoichiometry versus the time of reaction over skeletal nickel ( $m_{\text{Cat}} = 0.5$  g) in an aqueous solution of propan-2-ol with the alcohol mole fraction  $x_2 = 0.68$  ( $V = 10^{-4}$  m<sup>3</sup>): (a) without additives, (b) with the addition of sodium hydroxide (0.01 mol/L), and (c) with the addition of acetic acid (0.01 mol/L); lines are calculation and points are experiment ( $T = 303$  K,  $P = 1$  atm). The plot of the azoxybenzene amount versus time for the system containing sodium hydroxide was obtained by calculations.

**Table 2.** Rate constants corresponding to the optimum calculations by the model of nitrobenzene reduction on skeletal nickel in an aqueous solution of propan-2-ol ( $x_2 = 0.68$ )

Step	Rate constants of step*	Solvent		
		without additives	0.01 M CH <sub>3</sub> COOH	0.01 M NaOH
I	$k_1 \times 10^2, \text{m}^3 \text{mol}^{-1} \text{s}^{-1}$	$3.0 \pm 0.1$	$3.0 \pm 0.1$	$2.8 \pm 0.2$
	$k_1/k_2, \text{m}^3 \text{mol}^{-1}$	$3.8 \pm 0.2$	$3.8 \pm 0.2$	$3.8 \pm 0.2$
II	$k_3 \times 10^2, \text{m}^3 \text{mol}^{-1} \text{s}^{-1}$	$1.5 \pm 0.2$	$1.8 \pm 0.8$	$1.1 \pm 0.1$
	$k_3/k_4, \text{m}^3 \text{mol}^{-1}$	$0.4 \pm 0.2$	(0.1)	(1)
III	$k_5, \text{m}^3 \text{mol}^{-1} \text{s}^{-1}$	(0.5)	(0.05)	(0.5) **
	$k_5/k_6, \text{m}^3 \text{mol}^{-1}$	(1)	(1)	(10) **
IV	$k_7 \times 10^2, \text{m}^3 \text{mol}^{-1} \text{s}^{-1}$	(0.5)	(0.2)	(0.1)
	$k_7/k_8 \times 10^2, \text{m}^3 \text{mol}^{-1}$	(0.1)	(2)	(0.1)
V	$k_9, \text{kg mol}^{-1} \text{s}^{-1}$	(5)	$0.042 \pm 0.002$	(5)
	$k_{10}, \text{kg mol}^{-1} \text{s}^{-1}$	$5 \pm 1$	$2 \pm 0.03$	$5 \pm 1$
	$k_{11}, \text{kg mol}^{-1} \text{s}^{-1}$	$0.9 \pm 0.05$	$0.9 \pm 0.4$	(3)
VI	$k_{12} \times 10^2, \text{s}^{-1}$	$0.04 \pm 0.02$	(0.04)	$0.2 \pm 0.08$
VII	$k_{13} \times 10^3, \text{s}^{-1}$	$3.3 \pm 0.2$	—	$4.5 \pm 2$
	$k_{13}/k_{14}, \text{mol m}^{-3}$	7.3	—	7.3
VIII	$k_{15} \times 10^2, \text{kg mol}^{-1} \text{s}^{-1}$	$20 \pm 6$	$22 \pm 2$	$20 \pm 6$
	$k_{16} \times 10^2, \text{m}^3 \text{mol}^{-1} \text{s}^{-1}$	$2 \pm 0.8$	$0.15 \pm 0.03$	$2.0 \pm 0.8$

Estimated values are given in parentheses. Dashes in the columns mean that this step did not contribute noticeably to the overall reaction rate.

\* The dimensions of the constants depend on the dimensions of the concentrations.

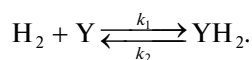
\*\* The constants were estimated using simulation because of the high rate of PHA conversion under the experimental conditions.

example, the rate of the catalyst surface oxidation ( $k_{14}$ ) can increase by a factor of 2–5. Probably, this is due to the increase in the rate of NS adsorption ( $k_3$ ). The experimental data indicate that the introduction of acetic acid into the solvent exerts almost no effect on the rate of NS adsorption ( $k_3$ ), decreases the rate of NS interaction with hydrogen in the surface layer ( $k_9$ ), and diminishes the contribution from the oxidation processes ( $k_{14}$ ).

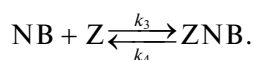
Unlike NS hydrogenation, the hydrogenation of NB proceeds via the formation of PHA, which is consistent with the opinion of Gelder [1] and with experimental data discussed in an earlier work [13]. According to that work [13], the stoichiometry of NB reduction does not correspond to the stoichiometry of the reaction with respect to hydrogen if the nitro group is completely converted to amine. Thus, catalyst surface oxidation during NB hydrogenation cannot be excluded.

The following sequence of steps was accepted for the conversion of NB on the basis of the above data.

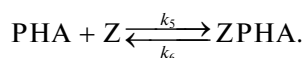
I. Hydrogen adsorption on the catalyst surface:



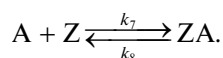
II. Adsorption of NB on the catalyst surface:



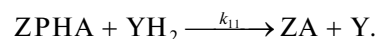
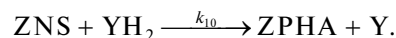
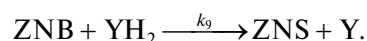
III. Adsorption of PHA on the catalyst surface:



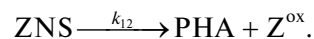
IV. Adsorption of A on the catalyst surface:



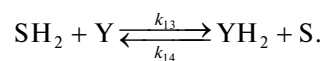
V. Chemical interaction in the surface layer:



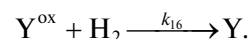
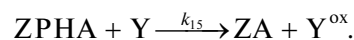
VI. Formation of oxidized sites Z:



VII. Reversible dehydrogenation of the solvent:



VIII. Formation of oxidized sites Y and their reduction:



The constants  $k_1$  and  $k_{13}$  and the ratio  $k_7/k_8$  were estimated from experimental data. The constant  $k_7$  and the ratios  $k_1/k_2$  and  $k_{13}/k_{14}$  were taken from earlier works [10, 11]. The constants  $k_5$ ,  $k_6$ ,  $k_{10}$ ,  $k_{11}$ ,  $k_{15}$ , and  $k_{16}$  were found earlier for the description of PHA and NS hydrogenation [14]. The constants  $k_3$ ,  $k_4$ ,  $k_9$ , and  $k_{12}$  were varied and were determined by the simulation of NB hydrogenation in an aqueous solution of propan-2-ol without additives. The values of the constants at which the calculation variant was optimal are given in Table 2.

The analysis of the results obtained for different kinetic schemes shows that the oxidation of the sites Z by the starting NB is hardly probable, because the contribution from this step is overlapped by the contribution from the oxidation of the sites Z with the intermediate reduction product (nitroso compound). The simulation results also indicate that NB is predomi-

nantly converted via PHA, whereas the formation of AZOB is unlikely.

The influence of acetic acid or sodium hydroxide introduced into the solvent was analyzed by comparing the optimum calculation variant for an aqueous-alcohol medium without additives with variants in which the rate constants of steps II, III, V, and VI corresponding to the adsorption of NB and PHA, their chemical interactions with adsorbed hydrogen, and the oxidation of the active sites Z, respectively, were varied.

The curves in Fig. 2 illustrate different variants of the calculations according to the proposed model.

The calculations showed that the introduction of sodium hydroxide into the aqueous solution of propan-2-ol favored an increase in the extent of irreversible oxidation of the sites Z. On the contrary, acetic acid decreases the constant of this step. The rate constant characterizing the reversible oxidation of the sites Y remained unchanged for all compositions of the solvents used.

Thus, the results of this study made it possible to propose kinetic schemes and to calculate the rate constants of nitro- and nitrosobenzene conversion steps taking into account the accompanying processes, such as catalyst surface oxidation and solvent dehydrogenation, as well as the competitive character of the adsorption of the starting compound and reaction product. The values of the rate constants obtained can be used in the development of kinetic models for other substituted nitrobenzenes.

The analysis of different variants of calculations confirmed the enhancement of the oxidation of the catalyst surface during the hydrogenation of nitrobenzene and especially nitrosobenzene in aqueous solutions of propan-2-ol containing sodium hydroxide. Conversely, the introduction of acetic acid into the solvent exerts a favorable effect and makes it possible to exclude the irreversible oxidation of the active sites of the catalyst surface. Thus, the theoretical calculations agree well with both the experimental data and theoretical assumptions discussed earlier [10, 12–14].

The simulation results suggested that the adsorption of the reaction product (aniline) on the oxidized surface of skeletal nickel was significantly worse than that in the absence of oxidation. The maximum in the

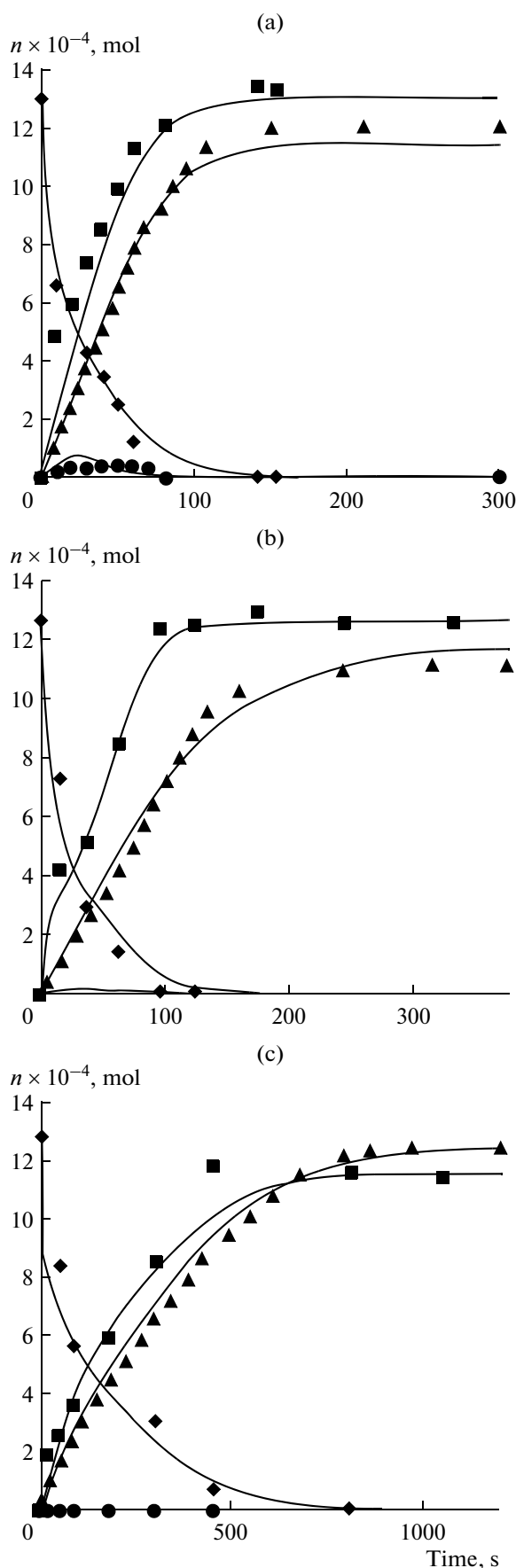


**Fig. 2.** Amounts of (◆) nitrosobenzene, (●) phenylhydroxylamine, (■) aniline, and (▲) hydrogen absorbed from the gas phase taking into account the stoichiometry versus the time of reaction over skeletal nickel ( $m_{\text{Cat}} = 0.5 \text{ g}$ ) in an aqueous solution of propan-2-ol with the alcohol mole fraction  $x_2 = 0.68$  ( $V = 10^{-4} \text{ m}^3$ ): (a) without additives, (b) with the addition of sodium hydroxide (0.01 mol/L), and (c) with the addition of acetic acid (0.01 mol/L); lines are calculation and points are experiment ( $T = 303 \text{ K}$ ,  $P = 1 \text{ atm}$ ). The plot of the phenylhydroxylamine amount versus time for the system containing sodium hydroxide was obtained by calculations.

kinetic curves of the time dependence of the aniline amount becomes less pronounced or disappears completely. This assumption is consistent with the previous opinion [10].

#### ACKNOWLEDGMENTS

This work was supported by the Ministry of Education and Science of the Russian Federation (state program no. 1800).

#### REFERENCES

1. Gelder, E.A., *PhD Thesis*, Glasgow: Univ. of Glasgow, 2005.
2. Manisha J. Vaidya, Shrikant M. Kulkarni, and Raghunath V. Chaudhari, *Org. Process Res. Dev.*, 2003, vol. 7, no. 2, p. 202.
3. Vinogradov, S.V., Ulitin, M.V., and Lefedova, O.V., *Russ. J. Phys. Chem.*, 1999, vol. 73, no. 11, p. 1741.
4. Budanov, M.A., Ulitin, M.V., Lefedova, O.V., and Nguen Tkhi Tkhu Kha, *Russ. J. Phys. Chem. A*, 2010, vol. 84, no. 11, p. 1901.
5. Lamy-Pitara, E., N'Zemba, B., Barbier, J., Barbot, F., and Miginiac, L., *J. Mol. Catal. A: Chem.*, 1999, vol. 142, p. 39.
6. Budanov, M.A., *Cand. Sci. (Chem.) Dissertation*, Ivanovo: Ivanovo State Univ. of Chemistry and Technology, 2012.
7. Kiperman, S.L., *Usp. Khim.*, 1978, vol. 47, no. 1, p. 3.
8. Romanenko, Yu.E., Lopatkin, E.V., Komarov, A.A., and Lefedova, O.V., *Izv. Vyssh. Uchebn. Zaved., Khim. Khim. Tekhnol.*, 2010, vol. 53, no. 8, p. 33.
9. Barbov, A.V., Ulitin, M.V., Shalyukhin, V.G., and Gostikin, V.P., *Zh. Prikl. Khim.*, 1993, vol. 66, no. 3, p. 497.
10. Nguen Tkhi Tkhu Kha, Lefedova, O.V., and Merkin, A.A., *Russ. J. Phys. Chem. A*, 2013, vol. 87, no. 4, p. 571.
11. Barbov, A.V., Shepelev, M.V., Filippov, D.V., and Ulitin, M.V., *Russ. J. Phys. Chem. A*, 2010, vol. 84, no. 9, p. 1605.
12. Merkin, A.A., Komarov, A.A., and Lefedova, O.V., *Izv. Vyssh. Uchebn. Zaved., Khim. Khim. Tekhnol.*, 2014, vol. 57, no. 1, p. 3.
13. Lefedova, O.V., Nguen Tkhi Tkhu Kha, Merkin A.A., and Komarov A.A., *Izv. Vyssh. Uchebn. Zaved., Khim. Khim. Tekhnol.*, 2012, vol. 55, no. 11, p. 31.
14. Romanenko, Yu.E., Komarov, A.A., Budanov, M.A., and Lefedova, O.V., *Izv. Vyssh. Uchebn. Zaved., Khim. Khim. Tekhnol.*, 2013, vol. 56, no. 6, p. 28.

*Translated by E. Yablonskaya*